Hindawi
Journal of Sensors
Volume 2022, Article ID 9395396, 14 pages
https://doi.org/10.1155/2022/9395396

*Research Article*

# Inverter Design and Droop Parallel Control Strategy Based on Virtual Impedance

**Lu Wang**

*School of Mathematics and Information Engineering, Chongqing University of Education, Chongqing 400065, China*

Correspondence should be addressed to Lu Wang; wanglu@cque.edu.cn

Received 20 January 2022; Revised 16 February 2022; Accepted 21 February 2022; Published 11 March 2022

Academic Editor: Wen Zeng



The present work is aimed at improving the performance of the multiobjective energy parallel step-by-step power generation system and enhancing the reliability and stability of the energy supply. Firstly, the difficulties of the ring current control method of the inverter power supply are summarized. Secondly, the causes of ring current in the circuit are analyzed. On this basis, the topology structure of the primary circuit of the inverter unit is designed, and the simulation model of the droop control is proposed for the inverter power supply. Finally, experiments are implemented to test the performance of the model. The results demonstrate that the waveform quality of the output voltage of the parallel system controlled by the virtual impedance technology is significantly improved. Specifically, the harmonic content near the fundamental wave significantly decreases compared with the original, from 6% to about 2%. Besides, the interference of the ring current to the parallel control inverter of the power supply system is weakened, and the output stability of the inverter power supply is improved. This study designs the structure of the inverter converter based on multiobjective decision-making and discusses the droop parallel control strategy. It provides a specific reference for controlling the circuit parallel system and has positive promotion significance for sustainable energy management and the rational utilization of electric energy.

## 1. Introduction

As the basis for the survival and development of human society, energy has always been the focus of research in related fields in various countries. With the rapid growth of the consumption of fossil fuels, such as oil and natural gas, all countries in the world are facing severe challenges in terms of energy consumption and environmental pollution [1, 2]. The widespread use of fossil fuels has caused severe damage to the ecological environment, indirectly affecting human development. At present, China's energy structure has many flaws. Coal energy consumption accounts for the most significant proportion of all primary energy resources, followed by oil, natural gas, hydropower, and nuclear power [3, 4]. It can be seen that China's energy consumption structure is very unreasonable, and the proportion of clean energy and the renewable energy consumption is much smaller than that of fossil energy [5]. Therefore, developing and improving the utilization efficiency of new energy and renewable energy is inevitable to solve the current global energy crisis. Electricity is the most popular energy form at present, which is cleaner and more convenient, playing the role of the lifeline of human society.

Energy shortage and environmental degradation are major issues faced by all countries worldwide for social development [6, 7]. Improving energy efficiency, accelerating the development of environmentally friendly, clean, and renewable energy, and strengthening the use of renewable energy are important choices in the national energy strategy. The development and utilization of renewable energy are fundamental for implementing the scientific development concept, building a resource-saving society, and achieving sustainable development [8]. It is also an important measure to protect the environment and deal with climate change. Distributed power generation has the advantages of saving energy, environmental protection, high efficiency, and flexibility, becoming the focus of relevant research fields worldwide. The distributed generation system with multiple power sources in parallel plays a vital role in promoting the development and utilization of renewable energy, expanding the capacity

of the power supply system, and improving the reliability of the power supply [9, 10]. The distributed power system has the following characteristics. First, the power source can configure various power sources through the power conversion network. Second, all distributed power sources are connected to the alternating current (AC) grid bus and play a role together. Third, a parallel inverter power supply is usually employed for small distributed generation systems. Fourth, the parallel connection of the inverter power supply does not require connecting wires, which is especially suitable for the inverter power supply to be connected to the power grid. An ideal distributed generation system consists of the parallel inverter power module, output line impedance, AC bus, and loads connected to the AC bus. Notably, the inverter power supply is the heart of the distributed generation system [11, 12]. It converts distributed energy sources into electricity through inversion, current sharing, and other techniques that enable the system to operate parallel with the grid. In the distributed generation of renewable energy, the inverter parallel connection control is critical in the parallel inverter system. The research on inverter parallel technology started late in China, and the parallel control study is immature. Most parallel systems use distributed control. This method has the great advantage that when there is a failure in the parallel system, the system will be automatically exited, effectively improving the system reliability. Connecting each module in parallel is suitable for current sharing control, and the information exchange between the modules is carried out through interconnection. This control method improves the redundancy of the parallel system, thus significantly improving reliability. However, more parallel modules and the wiring distance will easily interfere with the interconnection signal. Removing the interconnection between inverters in a parallel system can eliminate the above defects and improve the system's reliability. However, this operation will cut off the information exchange between parallel modules, dramatically increasing the difficulty of control. At present, the realization and parallel control of inverter modules is a hotspot in microgrid research. Nowadays, growing power equipment has begun to use unique power supplies. Paralleling the power supplies of the inverter power system can effectively improve the quality and efficiency of the power supply and prevent grid pollution, which has far-reaching significance. Some achievements have been made in researching inverter paralleling technology, but there are still many problems. Related research in China is in its infancy. The research on parallel control technology enables inverters to operate stably in parallel, which is of great practical significance.

Therefore, the present work firstly analyzes the parallel ring current control method of the inverter power supply and clarifies the difficulties of ring current control. Secondly, the ring current causes are analyzed to propose a corresponding current sharing control scheme based on the parallel system. The system control ideas are described in detail and comprehensively from the perspectives of central circuit topology, output characteristics and power control, inverter voltage synthesis, and power system monitoring of wireless parallel inverters. In addition to the digital simulation of the parallel control strategy of the inverter power supply, an experiment is designed to test its performance, hoping to achieve satisfying research results.

## 2. Literature Review

Lin et al. [13] designed an improved virtual impedance consisting of a resistor tuned by active deviation and a complex impedance component adjusted by a reactive variation to achieve accurate power distribution. They found that the droop control would cause system voltage amplitude and frequency deviations under steady-state conditions. The low-pass filter in the power calculation loop would reduce the system's dynamic performance. Peng et al. [14] combined the improved particle swarm optimization with virtual impedance. They used the algorithm to find the optimal parameters in the coupling compensation so that the system could guarantee a stable operating state. However, experimental results showed that introducing this algorithm would lead to poor dynamic performance. Chen et al. [15] proposed a two-level adaptive virtual impedance control scheme. The authors adjusted the active power through the maximum power bus in the first-level control to ensure the power-sharing of the system; they utilized the second-level control to eliminate the shared errors for active power, unbalanced power, and harmonic power. Zhang et al. [16] proposed an enhanced proportional power distribution strategy based on the adaptive virtual impedance to solve the power coupling in complex impedance environments. However, introducing a central controller resulted in time delay and signal error. Geng et al. [17] studied the resistive microgrid and adopted the method of virtual negative reactance control and adaptive virtual resistance. In this way, they eliminated the coupling between the active and reactive power of the inverter and realized distributed "plug and play" for power inverters. Liu et al. [18] introduced virtual impedance into the circuit to improve line impedance characteristics and solve the problem of system output power coupling. Still, they proved that virtual impedance would reduce the standard bus voltage.

Here, based on the parallel connection of two inverters, the equivalent output impedance of the parallel inverter system is shaped by introducing and designing the value of virtual complex impedance to realize power decoupling. In addition, an improved droop control method is proposed based on the original virtual impedance control. This scheme furnishes the parallel inverter system with a fast dynamic response speed, realizes good power sharing, and compensates for the voltage drop caused by the introduction of virtual impedance. Consequently, the system frequency deviation is within the controllable range, and the system frequency remains stable. Figure 1 displays the research framework.

## 3. Theory and Method

*3.1. Parallel Circulation Control Method for Inverter Power Supply.* The research on parallel inverter control technology began in the early 1980s. The rapid development of computer technology promotes the continuous innovation of power and electronic technologies, and research has also

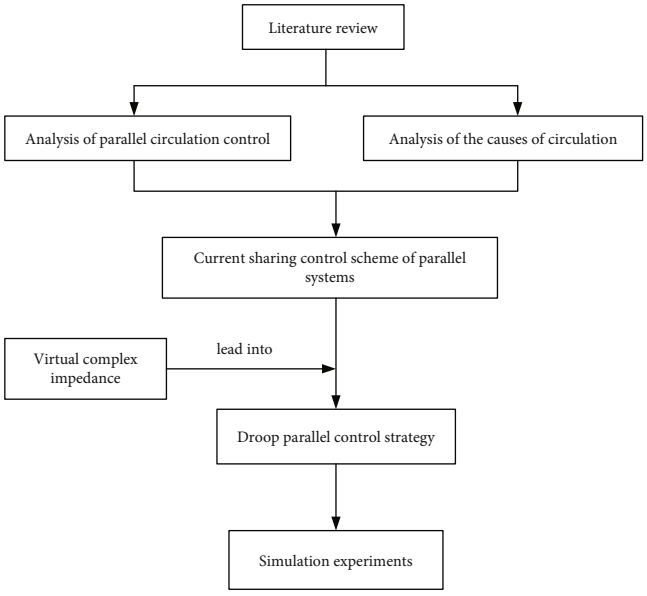


Figure 1: Research route.

made significant progress in inverter technology. In the field of inverter technology, parallel AC power supply has attracted increasing attention. The success of control schemes and concrete products has set a crucial benchmark for the high-performance development of parallel inverter power systems [19, 20]. Parallel inverter operation is deeply studied based on the successful experience of paralleling process. However, the inverter power supply outputs AC varying according to the sine wave law. Therefore, the parallel operation is more complicated than the parallel direct current (DC) power supply, primarily manifested in three aspects.

First, the inverter's voltage frequency and phase should be strictly synchronized, which is the premise to ensure that the inverter with the same capacity outputs the same active power when running in parallel [21, 22]. However, it is a great challenge to ensure voltage, frequency, and phase synchronization. Even if the voltage and frequency are consistent, a slight phase difference will cause serious balance problems for the output of active power of inverter voltage [23]. The smaller the output power, the greater the influence of phase difference on the inverter power supply. In more severe cases, rectification may even occur.

Second, the output voltage amplitude will be uneven after the phase and frequency are synchronized, generating many reactive circulating current components at the output current. The consistency will also increase the loss of the inverter and even lead to power overload burning the power supply [24].

Third, after the output voltage of each inverter in parallel operation reaches sinusoidal waveform, indicating that the frequency, phase, and amplitude are the same, the inverter output will also affect the difference of harmonic components of each output voltage and generate parallel units between harmonic circulation.

Therefore, to meet the operation requirements of the inverter, the frequency, phase, amplitude, and waveform height of the output voltage of each parallel unit need to be consistent, and the load current should be reasonably distributed [25]; the former is aimed at solving the problem of voltage phase waveform synchronization.

There are two typical ring current suppression methods for parallel operation of inverters: the coupling inductance method and the isolation transformer method.

When the output voltages of the two inverters are inconsistent, the coupled inductance method will produce circulating current flowing between the two inverters without passing through the load $\dot{I}_H$. Assuming that the inductors $L1$ and $L2$ are completely coupled, the size of the ring current is

$$\dot{I}_H = \frac{\dot{I}_{o1} - \dot{I}_{02}}{2} = \frac{\dot{U}_{o1} - \dot{U}_{o2}}{2R + 4jX}, \tag{1}$$

where $R$ represents the line resistance from the output terminal of the inverter voltage to the load, $\dot{U}_{o1}$ and $\dot{U}_{o2}$ denote the output voltage of the two inverters and the voltage of the parallel bus bar, $L$ stands for the coupling inductance, and $jX$ refers to the inductive reactance. Since $R$ is much smaller than $L$, Equation (1) can be simplified as

$$\dot{I}_H = \frac{\dot{I}_{o1} - \dot{I}_{02}}{2} = \frac{\dot{U}_{o1} - \dot{U}_{o2}}{4jX}. \tag{2}$$

Equation (2) shows that the size of the ring current is inversely proportional to the inductance value of the coupled inductor, and the coupled inductor significantly reduces the ring current. Suppose that the number of turns of the inductors $L1$ and $L2$ is $N1 = N2 = N$; the two inductors are wound on the same iron core and are tightly coupled. When there is no ring current between the inverters, $\dot{I}_{o1} = \dot{I}_{02}$. The magnetic flux of the iron core can be expressed as

$$\phi = \frac{L1 * I_{o1}}{N1} - \frac{L2 * I_{o2}}{N2} = 0. \tag{3}$$

Equation (3) indicates that due to the coupling effect of the ring current suppression inductors, the magnetic fluxes of the two inductors cancel each other out, and the equivalent inductance value of the inductors is zero. Therefore, the inductors do not affect the voltage regulation accuracy. The advantage of coupled inductor method is that it has a good circulation suppression effect, can suppress active power, reactive power, and DC circulation, has small volume, and does not affect the voltage stabilizing accuracy of output voltage. However, it is challenging to wind the multimachine parallel-coupled inductor.

The principle of the isolation transformer method to suppress the ring current is relatively simple. In essence, it uses the isolation of transformers to disconnect the circulating current path. The isolation transformer method can eliminate the DC loop-current caused by the inconsistent DC components of the inverter output voltage. Meanwhile, the isolation transformer can electrically isolate the input DC voltage and output voltage of each inverter module,

improving the reliability of the parallel inverter system. The isolation transformer method has a good circulation suppression effect, can reduce active and reactive circulation, and eliminates DC circulation; besides, it is easy to connect in multimachine parallel. However, isolation transformers have bulky volumes and significantly affect the voltage stabilization accuracy of parallel circulation bars.

*3.2. Cause Analysis of Circulation.* The different output characteristics of inverter modules in distributed generation systems will generate a circulating current between inverters. The parallel system can operate normally only when the parallel inverter does not produce a circulating current and expected load current. The causes of circulating current are analyzed in this section to eliminate the ring current between inverters [26]. Figure 2 illustrates the equivalent circuit between the two inverters.

In Figure 2, $R3$ denotes the load impedance of the inverter power supply; $R1$ and $R2$ are the impedance of the inverter power supply line; $A_1$ refers to the current test; $I_1$, $I_2$, and $I_3$ represent the current corresponding to the three resistances, respectively; $\dot{I}_1$, $\dot{I}_2$, and $\dot{I}_0$ are the annular current in the corresponding circuit. When the output voltage waveform is sinusoidal and there is no waveform distortion, the relationship among $A_1$, $A_2$, and $A_3$ and $I_1$, $I_2$, and $I_3$ is described as

$$\begin{aligned} \dot{I}_1 &= \frac{\left(A_1 - \dot{A}_3\right)}{R_1}, \\ \dot{I}_2 &= \frac{\left(\dot{A}_2 - \dot{A}_3\right)}{R_2}, \\ \dot{I}_0 &= \dot{I}_1 + \dot{I}_2. \end{aligned} \tag{4}$$

Equation (5) defines the circulating current $\dot{I}_h$.

$$\dot{I}_h = \frac{\dot{I}_1 - \dot{I}_2}{2}. \tag{5}$$

Equations (6) and (7) are set up when the three resistance impedance values are equal.

$$\dot{I}_h = \frac{\left(\dot{A}_1 - A_2\right)}{2R} = \frac{\Delta\dot{A}}{2R}, \tag{6}$$

$$\begin{cases} \dot{I}_1 = \dfrac{\dot{I}_0}{2} + \dot{I}_h, \\ \dot{I}_2 = \dfrac{\dot{I}_0}{2} - \dot{I}_h. \end{cases} \tag{7}$$

Equations (6) and (7) show that when two inverters are connected in parallel, the output current of different equipment consists of two parts: the output current under load and the circulating current between two parallel power supplies [27, 28]. The load distribution of parallel equipment is uniform; the output current of parallel equipment is affected by the circulating current. Suppose the output of each unit is different from a load of voltage circulating current. In that case, the output power of each division will change accordingly, resulting in a load imbalance on each power supply of the inverter. The impedance in the electronic circuit is minimal. Suppose the phase and amplitude of the output voltage vector of each parallel unit are inconsistent. In that case, even the most minor difference will produce magnetic flux far greater than the rated current of the system [29]. This current flows through the two inverters between the loads. If two inverters controlled by a closed voltage circuit are connected in parallel at this time, it will cause a pseudo short circuit of the system, which is extremely dangerous [30]. Therefore, it is necessary to equalize the current of the inverter power supply running in parallel to evenly distribute the current and thermal stress between the power supply units to prevent multiple power supplies from being in the current limiting mode.

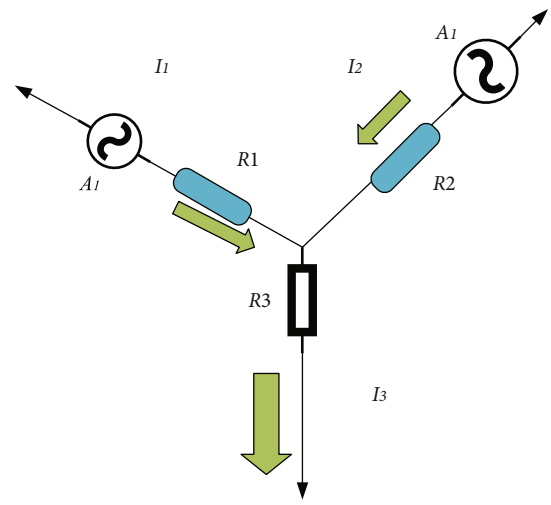


Figure 2: Equivalent parallel connection of two inverters.

*3.3. Current Sharing Control Schemes of Parallel System.* There are three common methods to balance the load current of inverter units in parallel systems: current sharing of series current limiting inductance, master-subsetting control, and maximum current automatic sharing. Figure 3 reveals the principle of current sharing of the series current limiting inductor method.

In the current sharing scheme of series current limiting inductors in Figure 3, Ua and Ub are the voltages across the inverter 1 and inverter 2, respectively; Uc is the voltage across the inductor; $R1$ and $R3$ are series resistance; $Rc$ is the inductor resistance; $L1$ and $L2$ are the inductors; $I1$ and $I2$ are the currents in the series circuit. When there is no current flowing between the inverters, the output currents of the two inverters are balanced. Since the output current flows through the two coils in the direction shown in Figure 2, the magnetic fluxes generated by the two currents cancel each other out; in this way, the equivalent inductance value is close to zero, reducing the impact on the system voltage regulation accuracy [31, 32]. When the

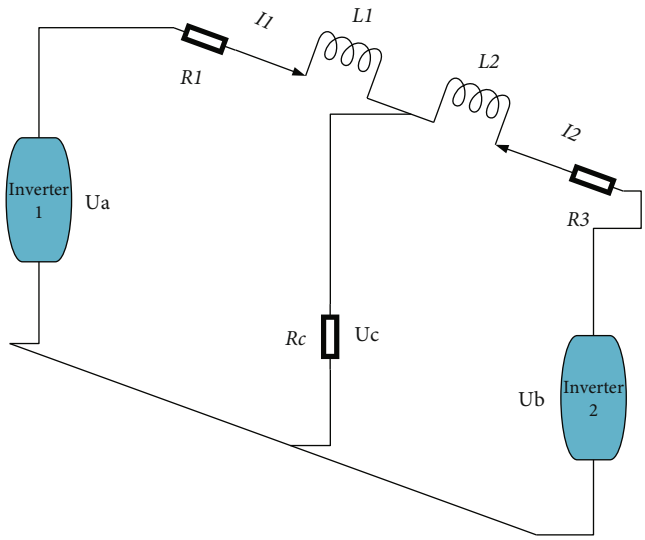


Figure 3: Current sharing of the series current limiting inductor.

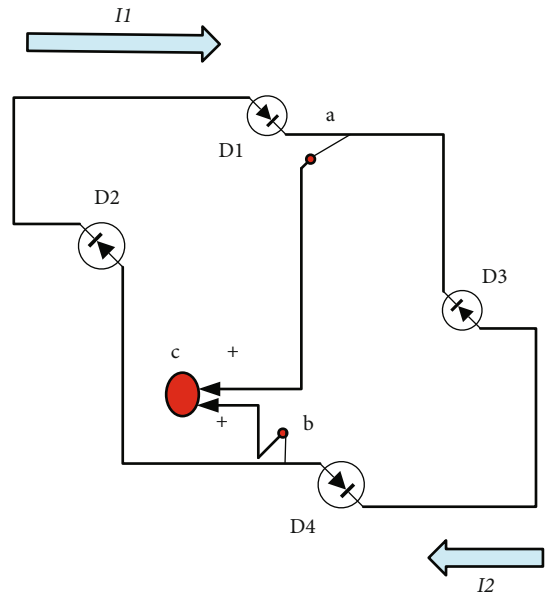


Figure 4: Automatic control principle of maximum current sharing.

current flows, the magnetic flux is caused by the increasing current, and the equivalent inductance value increases, effectively suppressing the ring current.

The master-subsetting control method is only applicable to parallel inverter systems with common current control types. Current control refers to the voltage-to-current dual control loop composed of the current loop as the inner loop and the voltage loop as the power module's outer loop [33, 34]. The parallel system adopts the master-subsetting to share the current, and the voltage-controlled inverting power supply and current-controlled inverting power supply are connected in parallel. In the parallel inverter, the "master module" is set to operate manually according to the voltage control law to control the output voltage of the parallel system to change sinusoidally [35, 36]. Other submodule devices run in the current control mode. Generate current in full accordance with the current command specified by the main module to eliminate the current flowing through the system effectively.

Figure 4 reveals the principle of automatic current sharing of maximum current.

In Figure 4, $I1$ and $I2$ are the output currents of the inverting power supply 1 and 2, respectively; $D1$ and $D3$ are the current controllers (current amplification) of the inverting power supply 1 and 2, respectively; $D2$ and $D4$ are voltage controllers (voltage amplification) of inverting power supply 1 and 2, respectively; $c$ stands for the maximum current output by the inverting power supply. The diode is unidirectional. This feature can ensure that the inverter unit with the most extensive output current turns on the diode and continuously transmits the maximum current of the unit to the bus. However, in this process, diodes will lead to a voltage drop at both ends, resulting in the failure of current sharing of the main module and a particular error, and the submodule will have better current sharing. In fact, there are many ways to realize the current sharing regulation, such as designing a unique hardware system to complete the current sharing or designing a special software to control the current sharing. Academic opinions are divided. Various current sharing methods will result in different stability and accuracy characteristics.

*3.4. Module Design of the Parallel System.* The parallel system of the inverter power supply is composed of multiple unit modules. The performance of different modules needs to be synchronized to ensure the effect and safety of use. Therefore, it is necessary to reasonably design the inverter structure and control strategy. Figure 5 shows the central circuit topology of the inverter unit designed here.

According to Figure 5, the topology of the primary circuit of the inverter unit is changed to integrate the parallel function of the inverter and the parallel system of the inverter power supply. The primary circuit of each parallel inverter unit adopts the main circuit of the full-bridge inverter. Without considering the equivalent series resistance of the filter capacitor, a filter is used to filter other bands in the bridge except for the higher harmonics of the output voltage.

In Figure 5, Vdc represents the DC input voltage of the system, $T1$-$T4$ denotes the power switch module, $L$ and $C$ stand for the output filter inductance and capacitance of the system, $R1$ refers to the equivalent series resistance of the filter inductance, and $R2$ signifies the system load. Equation (8) describes the frequency domain function between the voltage between points $A$ and $B$ and the output of the inverter unit.

$$G(s) = \frac{R2}{RLC^2 + (L + R1R2C) + (R2 + R1)}. \tag{8}$$

*3.5. Droop Parallel Control Strategy of Inverter.* The parallel operation of the inverter power supply requires corresponding preconditions, and each parallel unit must be placed on

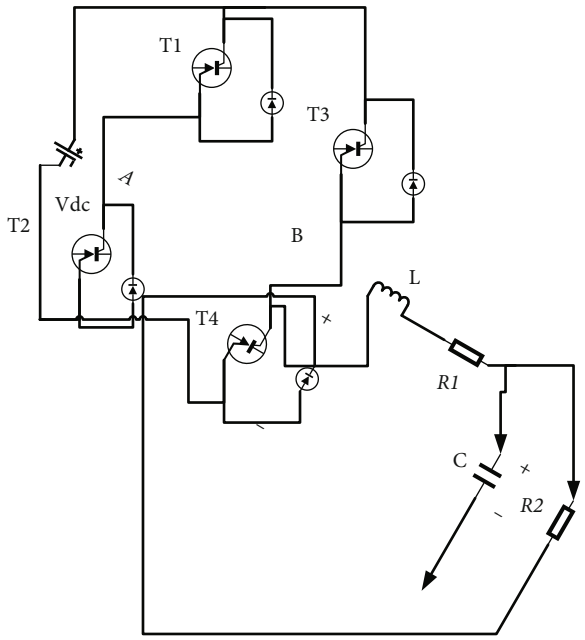


Figure 5: Main circuit topology of the inverter unit.

the AC bus network. At the beginning of the process, the frequency, phase, and amplitude of output voltage shall be consistent with that of the AC bus. Significant phase and amplitude differences will produce large active and reactive loop currents during operation. These currents may dramatically impact the stable operation of the AC bus and system and cause an overcurrent of the inverter power supply, ultimately damaging the inverter power supply. The inverter must be designed in the concrete plan to terminate the parallel operation automatically. During the operation of the inverter, there is a presynchronization process to ensure that the phase, frequency, and amplitude of the inverter power supply are consistent with the power grid. It also reduces the impact on the power supply of the microgrid and inverter itself. The phase-frequency tuning process of the inverter unit before the parallel operation is called parallel presynchronization of the inverter unit.

According to the power characteristics of the above parallel inverter system, some researchers have proposed a control technology that can wirelessly parallel inverter, namely, the voltage frequency droop method. The parallel inverter device can sense the output power of the power supply system, measure and adjust the output voltage, frequency, and amplitude control values through droop control, and obtain the system's active power and total reactive power. The output frequency and the active output power of the inverter with large output active power decrease due to the frequency drop characteristics. When the inverter outputs low active power, the output frequency increases due to the frequency reduction characteristics, increasing active power. The voltage amplitude of the inverter outputting ample reactive power decreases due to amplitude decrease, reducing the reactive power output. The voltage amplitude increases for the inverter with small reactive output power,

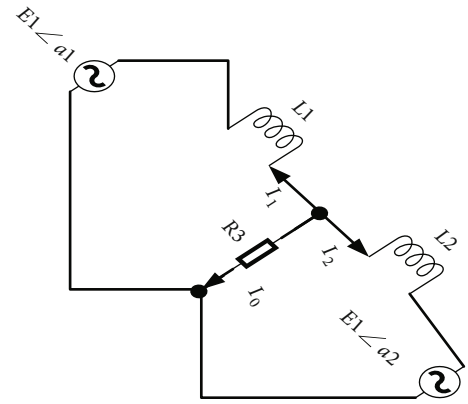


Figure 6: Equivalent circuit of the parallel system.

and the reactive output power decreases due to the amplitude decreasing characteristic. In other words, the equipment with low output power will increase the output according to the voltage frequency droop characteristics. In contrast, the relatively high output power equipment will reduce the output power. This self-regulation process is repeated in the parallel system until the minor loop point in the circuit is found.

The distributed generation system composed of parallel inverters has a complex structure. The AC voltage output by each inverter power supply is equivalent to a voltage source with mutually adjustable and controllable frequency, phase, and amplitude, and each unit shares the load current. In the distributed generation system, the line resistance is low, and the line impedance is inductive, which significantly simplifies the equivalent circuit of the parallel system, as shown in Figure 6.

Equation (9) signifies the negative power expression of the output power supply.

$$\begin{aligned}\bar{S}_i = P_i + jQ_i = \vec{E}\vec{I}_i^{*} &= E\left[\frac{E_i \cos a_t + \mathrm{j}E_i \sin a_i - E}{jX_i}\right]^{*} \\ &= \frac{E_1 E}{X_t} \sin a_t + j\left[\frac{E_t \mathrm{E}\cos a_i - E^2}{X_i}\right].\end{aligned} \tag{9}$$

In Equation (9), $\bar{S}_i$ represents the negative power of the output power supply; $P_i$ and $Q_i$ denote the active power and reactive power transmitted by the line, respectively; $a$ refers to the angle between the output voltage vector of the inverting power supply $E_i$ and the system output voltage vector $E$; $X_i$ indicates the output reactance of the inverting power supply.

Equation (10) reveals the output active power of each inverter in the equivalent circuit.

$$P_1 = \frac{E_1 E}{X_i} \sin \delta. \tag{10}$$

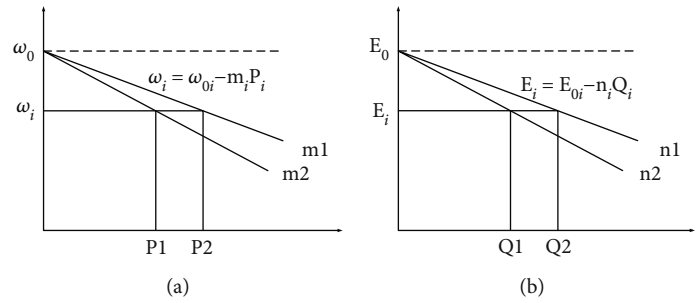


Figure 7: Droop inverter with different capacities: (a) active power; (b) reactive power.

In Equation (10), $\delta$ represents the phase difference. Accordingly, Equation (11) demonstrates the output reactive power of each inverter in the equivalent circuit.

$$Q_i = \frac{E_i E \cos \delta_i - E^2}{X_i}. \tag{11}$$

Because the power output of parallel system $E$ is strictly limited in practical application, it will not fluctuate wildly. Thus, the power output can be regarded as a constant approximately. Output impedance $X_i$ is also a fixed value. Hence, Equations (10) and (11) can be simplified as

$$P_i = k \sin a, \tag{12}$$

$$Q_i = kE_i - b, \tag{13}$$

where $k$ is the proportional coefficient and $b$ is a constant. Equations (12) and (13) demonstrate that the active power depends on the value of the angle $a$ between the inverter output voltage vector $E_i$ and the system output voltage vector $E$. In contrast, the reactive power mainly depends on the value of the inverter output voltage vector $E_i$.

Because the internal resistance of the inverter is meager and the external output characteristics are complex, even a tiny difference in amplitude or phase will cause a large system cycle between the inverters. The present work uses the parallel voltage frequency droop method for control. The frequency and amplitude of the output voltage of each inverter power supply are adjusted according to Equations (14) and (15) based on the droop method to make the output characteristics smoother.

$$\omega_1 = \omega_{0i} - m_i P_i, \tag{14}$$

$$E_i = E_{0i} - n_i Q_i. \tag{15}$$

In Equations (14) and (15), $P_i$ represents the active power, $Q_i$ refers to the reactive power, and $\omega_{0i}$ stands for the $i$th output angular frequency of inverter power supply under no load. $E_{0i}$ indicates the output amplitude of the first inverter under no load. $m_i$ denotes the droop coefficient of output angular frequency of the $i$th inverter power supply. $n_i$ denotes the droop coefficient of the output voltage amplitude of the $i$th inverter power supply. Figure 7 displays the scheme of droop inverter with different capacities.

Figure 7 presents the scheme of drooping characteristics when two inverters with different capacities are connected in parallel. Each inverter power supply in Figure 6 adjusts the frequency and amplitude of each output voltage back to a new and stable output operating point and distributes the output power reasonably. The same vertical slopes in the droop inverter characteristic diagram of the inverting power supply mean that each supply has stable performance and equal output power. If the droop slopes are different, the force is small when the slope is significant and vice versa.

In essence, the droop voltage frequency method takes the whole system with parallel inverters as the research object and detects the frequency and amplitude of output voltage. Then, it adjusts the active and reactive power by fine-tuning the frequency and amplitude to realize the reasonable distribution of power. Voltage frequency droop control reduces the active output by lowering or increasing the frequency to improve the active output. Reducing the voltage amplitude can reduce the reactive power; increasing the voltage can increase the reactive power. In short, this is a dynamic continuous self-adjustment according to voltage-frequency droop characteristics. In this way, the system can operate in a state where the circulation is the smallest.

Next, a virtual impedance is introduced into the circuit. In a low-voltage microgrid, the line impedance is primarily resistive. The system impedance is generally complex, and the resistance-inductance ratio in different systems is different, which is easy to cause power coupling. The method of introducing a virtual complex impedance can be adopted to solve the power coupling problem in the system. Besides, the value of the virtual complex impedance is designed according to the line impedance. The equivalent output impedance of the inverter is purely resistive or inductive, realizing the decoupled control of active power and reactive power. Figure 8 is a block diagram of the voltage and current double closed-loop control after introducing the virtual complex impedance.

In Figure 8, the virtual complex impedance $Z_v(s)$ consists of a positive virtual resistance $R_v$ and a negative virtual inductance $L_v$; $U*(s)$ refers to the voltage command value generated by the droop control module; $G_{PR}(s)$ and $G_i(s)$ are the transfer functions of the regulators in the voltage outer loop and the current inner loop, respectively; $K_{PWM}$

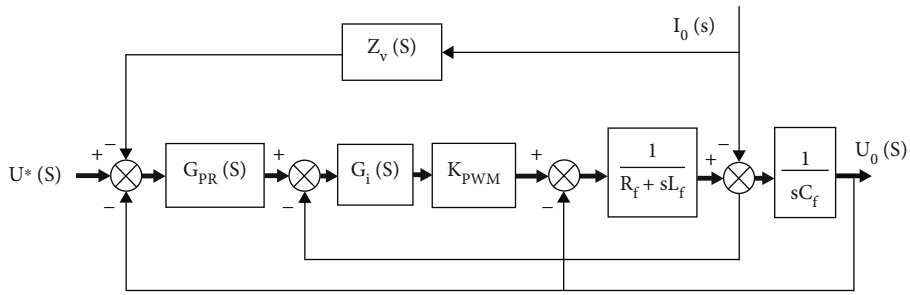


Figure 8: Block diagram of voltage and current double closed-loop control based on virtual complex impedance.

Table 1: System parameters.

| Project | Numerical value |
|---|---|
| LC filter | $R_f = 0.0485\,\Omega$, $L_f = 20\,\text{mH}$, $C_f = 20\,\mu\text{F}$ |
| Voltage control loop | $k_{vp} = 0.085$, $k_{vi} = 10$, $\omega_c = 10\,\text{rad/s}$ |
| Current control loop | $k_{ip} = 4.35$ |

is the pulse width modulation (PWM) gain of the inverter; $U_0(s)$ and $I_0(s)$ are the actual value of the inverter output voltage and the reference value of the output current, respectively; $R_f$, $L_f$, and $C_f$ represent the filter resistor, filter inductor, and filter capacitor in the low-pass filter, respectively.

The transfer functions of the quasiproportional voltage and current regulators can be defined as

$$\begin{cases} G_{PR}(s) = k_{vp} + \dfrac{2k_{vi}\omega_c s}{s^2 + 2\omega_c s + \omega_0{}^2}, \\ G_i(s) = k_{ip}. \end{cases} \tag{16}$$

In Equation (16), $k_{vp}$ and $k_{vi}$ denote the voltage loop's proportional gain and resonance gain, respectively; $k_{ip}$ represents the proportional gain of the current loop; $\omega_c$ refers to the corner frequency of the cutoff frequency. The LC filtering and voltage and current double closed-loop control parameters are designed, respectively, to smoothly realize the droop control of the low-voltage inverter parallel system. The specific parameters are summarized in Table 1.

In this paper, after introducing the designed virtual complex impedance, the system impedance must be approximately resistive at the fundamental frequency to adapt to the traditional droop control. Besides, it needs to be resistive at the harmonic frequency to meet the requirements of power decoupling and suppress the interharmonic and higher-order harmonics of the output current of the converter. The virtual impedance value is designed according to the line impedance $Z_n$ ($n$ *is* 1 or 2) (assuming $Z_n = 1\,\Omega + 2\,\text{mH}$) parameters in Table 1 to select the value range and the optimal impedance value is determined according to the impedance angle change.

*3.6. Simulation and Experiment of Droop Parallel Control.* Figure 9 indicates the simulation model of the droop control inverter proposed here.

Figure 9 suggests that the primary circuit model of the inverter can be combined with the control strategy through the connection of controlled variables to establish the simulation model of the wireless parallel system of the inverter. Parallel inverter theory is developed with the following parallel control theory as the core. Therefore, the proper application of droop theory is the premise of the system's regular operation.

The parameter settings of the simulation model of the parallel inverter power system reported here are shown in Tables 2 and 3.

Due to the limited detection accuracy of voltage amplitude, voltage frequency, deflection coefficient, hardware circuit, and software control accuracy, it is difficult to match each inverter's actual values of controlled variables completely. When the parallel controlled variables do not check, it is critical to judge the stability of the performance of the connected system.

## 4. Results and Discussion

*4.1. Simulation Results of Droop Theory Application Experiment.* Figure 10 illustrates the simulation results of the parallel system when the parameters of the two inverters are the same.

In Figure 10, all parameters of the two inverters are assumed to be the same. The working state of the inverter parallel system under droop control is relatively stable. The output of active and reactive power is well separated and stably balanced. Each power supply provides half of the system's capacity, and the circulation defaults to zero. The results show that the droop theory can be applied to parallel inverter systems and achieve a good control effect under ideal conditions. The power loop theory believes that when the output impedance of the system accounts

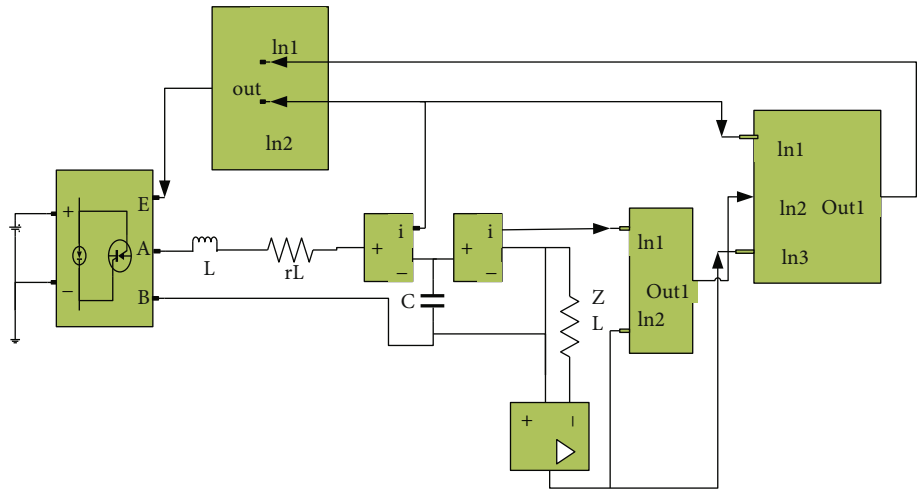


Figure 9: Simulation model of inverters controlled by the droop method.

Table 2: Parameters in the simulation system.

| System parameters | $L$ (mH) | $r$ ($\Omega$) | $C$ ($\mu$F) | $E$ (V) |
|---|---|---|---|---|
| Numerical value | 1 | 0.01 | 30 | 165 |

Table 3: System command parameters.

| Instruction parameter | Voltage (V) | Voltage frequency (rad) | Sag coefficient $m$ | Sag coefficient $n$ |
|---|---|---|---|---|
| Numerical value | 155 | 314 | 0.0001 | 0.0001 |

for a small proportion, the output impedance of the inverter is inductive in the entire frequency band. In other words, the output impedance of the system is not sensitive to the effect of the transition. The correct application of droop theory in the practical approach can be guaranteed to meet this point.

To further verify the inhibitory effect of circuit feedback on impedance $R$, set the impedance $R$ of inverter 1 to 0.01 $\Omega$ and the impedance $R$ of inverter 2 to 0.1 $\Omega$. Figure 11 presents the simulation results of parallel operation with a 6.0 $\Omega$ impedance load under the condition of consistent other parameters.

According to Figure 11, when the impedances of the two inverters are different, the parallel system under droop control works stably, and the active power and reactive power are also stable and balanced. Through the feedback of induced current, they tend to zero. The results suggest that the circuit feedback of the inductor can reduce this effect. Therefore, when the two inverters work in parallel under different conditions, the droop control can continue to apply and obtain satisfying control efficiency.

*4.2. Analysis of System Performance.* Droop control plays a role in practical application, but it also has limitations. A parallel self-tuning virtual impedance strategy is proposed here. By improving the droop parallel control, the system can improve the dynamic tuning performance, steady-state output frequency performance, and harmonic suppression to a certain extent. Figure 12 reveals the comparison of systematic dynamic adjustment characteristics before and after improvement.

As Figure 12 reveals, the parallel system of the inverting power supply is dynamically adjusted. The experimental conditions and parameters of the parallel system are the same as those of the simulation experiment, which means that the simulation system will produce periodic current waveforms. Figure 12 bespeaks that adding differential regulation to the power droop control of the system can significantly improve the dynamic regulation rate, speed up the power convergence, and improve the performance of the dynamic approach to a certain extent. Meanwhile, with the introduction of automatic control, even if the control voltage is different from the ring current of the original design, the ring current of the system is adequately controlled due to the compensation of the virtual impedance to the system. The command voltage of the whole system is significantly reduced only in the steady state, and the steady-state and dynamic performance is improved dramatically.

Figure 13 presents the active output frequency of the system.

Figure 13 signifies the comparison results of the active output frequency of the traditional droop parallel system and the droop automatic adjustment output frequency. It

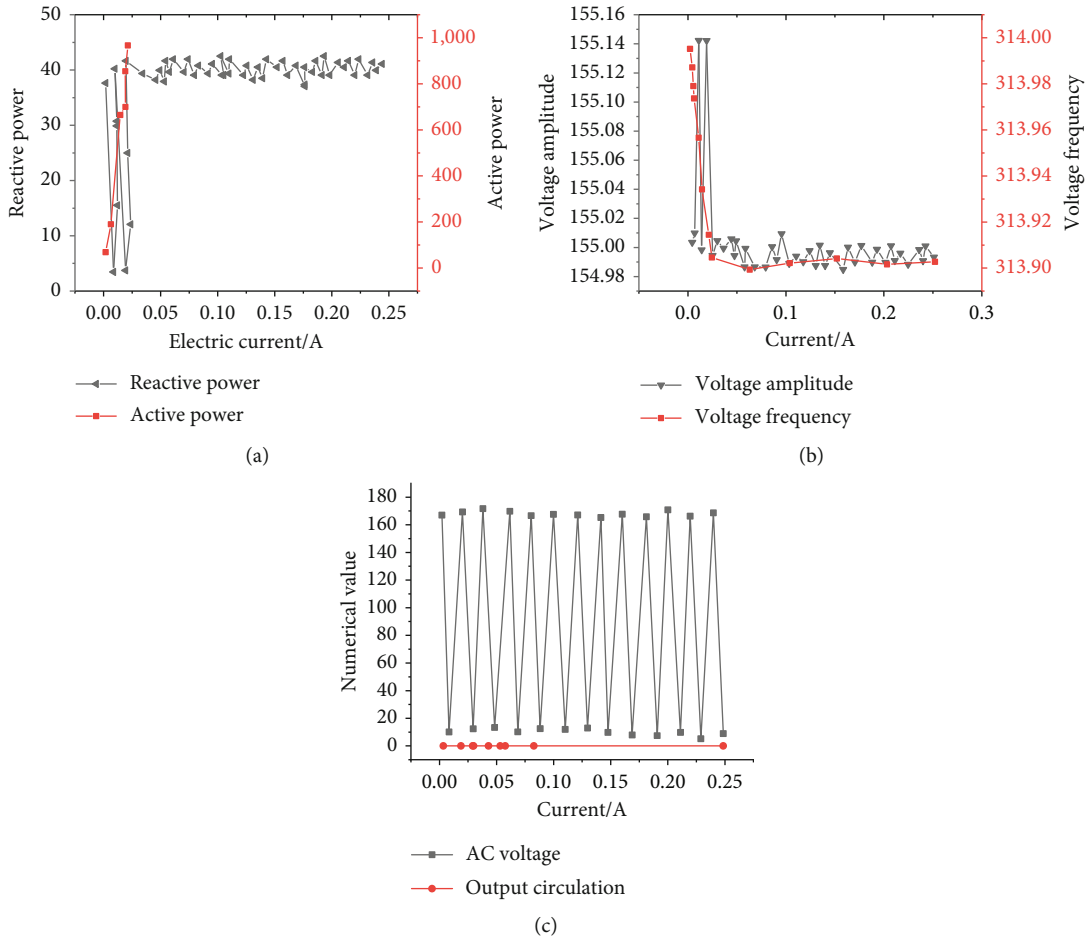


Figure 10: Simulation results of consistent inverter parameters: (a) power; (b) voltage; (c) frequency.

also implies that the conventional control method is adopted. The output frequency deviates from the control signal when the system reaches a stable state. When AC is connected to the grid, if the deviation is significant, it cannot meet the frequency requirements, which greatly limits the power range of the inverter. By dynamically adjusting the active power droop coefficient, the steady-state output frequency. Therefore, the system shows a small oscillation close to the driving frequency, which undoubtedly achieves the steady-state performance of the output frequency. Secondly, the dynamic response time of the system is hardly affected. The active power reduction factor can improve the steady-state index of the parallel system without affecting the dynamic performance of the system.

Figure 14 signifies the nonlinear load performance of the system.

Figure 14 reveals that both simulation systems are equipped with two bridge rectifier loads. It also implies that the waveform quality of the output voltage of the parallel system controlled by the virtual impedance technology has been significantly improved. Besides, the harmonic content near the fundamental wave is considerably lower than the original, from 6% to about 2%, declining four percentage points. Therefore, virtual impedance technology can successfully apply droop theory to nonlinear loads and expand the scope of the parallel inverter system.

To sum up, two simulation tools are used to analyze the main circuit and control circuit of the unit module of the parallel system. Simultaneously, according to the specific requirements of the parallel function of the inverter, the output power measurement and unit calculation are carried out. Based on the function of parallel and control voltage synthesis, construction is implemented on a complete application simulation model of an inverter wireless parallel system. The dynamic and static simulation experiment of the fully connected droop control system fully reflects the accuracy and feasibility of the control theory. Moreover, the experimental comparison is made on the application simulation models of two groups of parallel systems with different control strategies. Compared with the conventional droop parallel control strategy, the control strategy in this study shows noticeable improvement in the dynamic performance and steady-state index of the system. The simulation model of a parallel wireless inverter system established here provides an experimental platform for future system theory research.

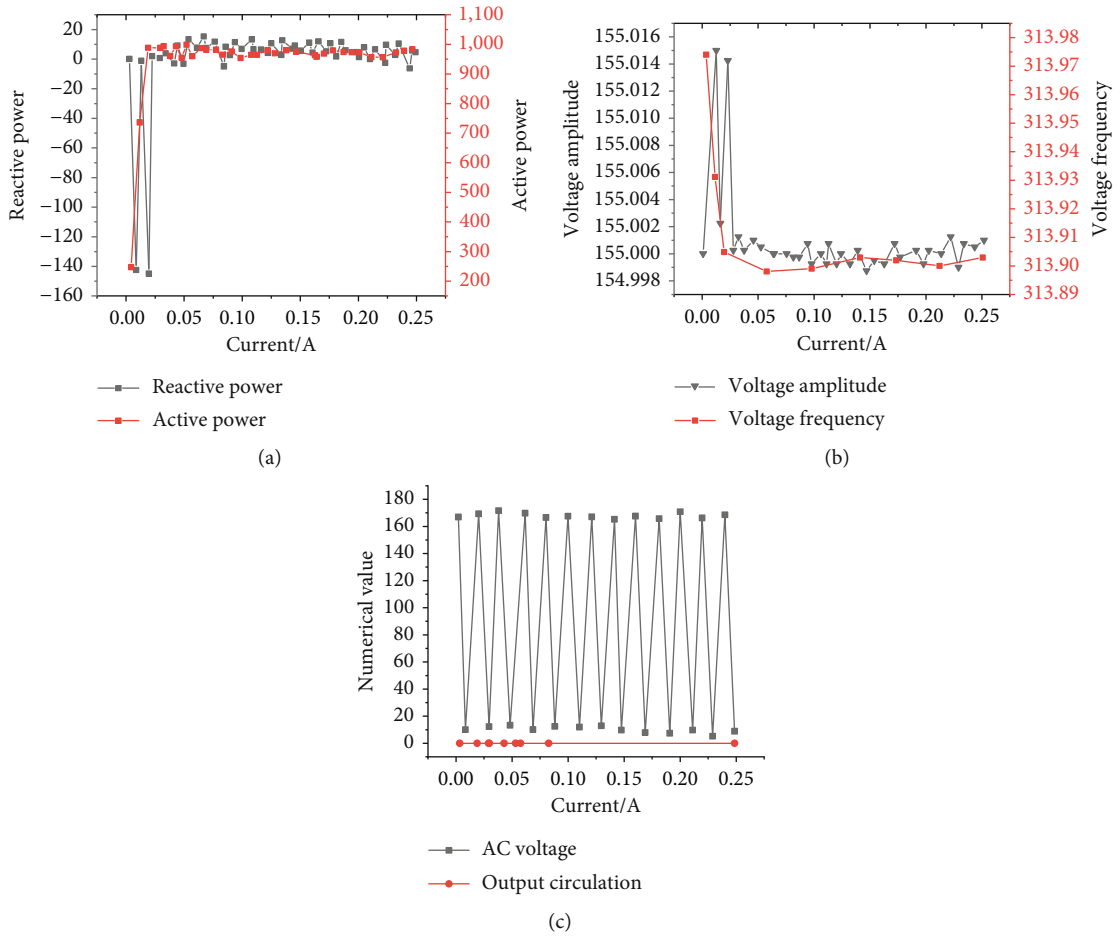


Figure 11: Simulation results of the parallel system with a different impedance of inverting power supply: (a) power; (b) voltage; (c) frequency.

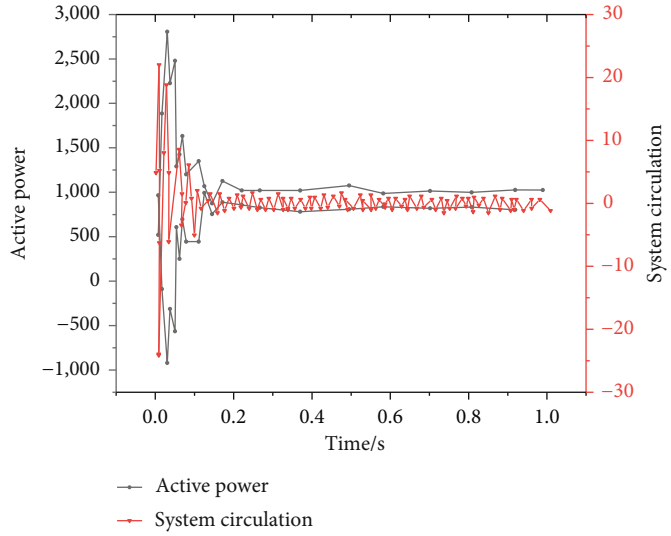


Figure 12: Comparison of systematic dynamic regulation characteristics.

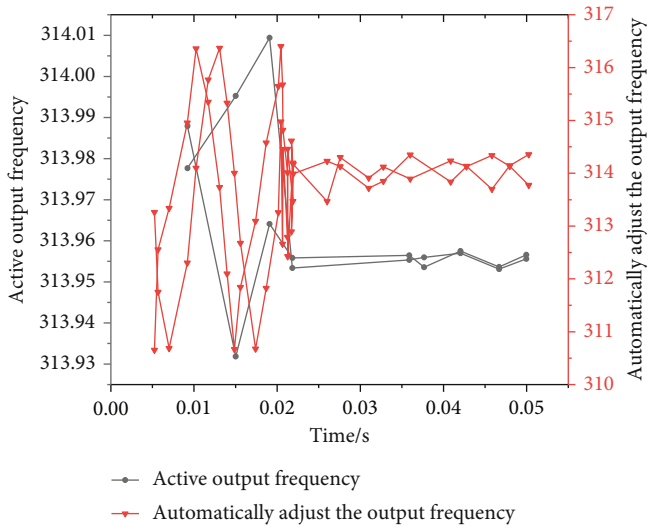


Figure 13: Active output frequency of simulation system.

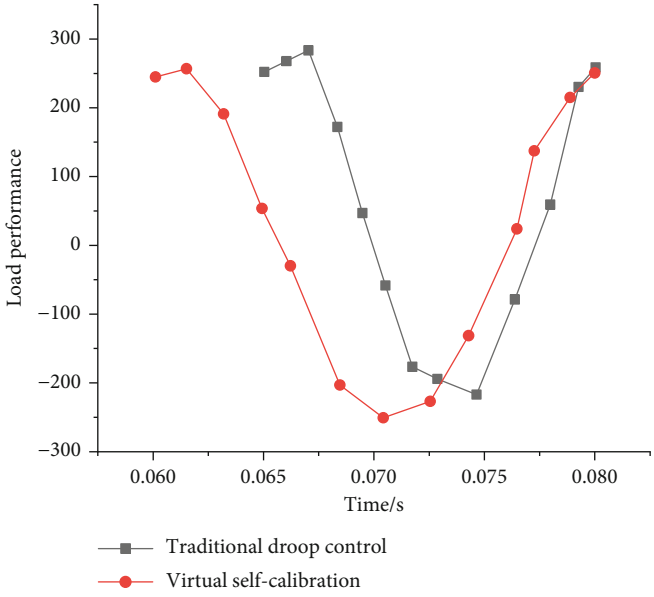


Figure 14: Comparison of system nonlinear load performance.

## 5. Conclusion

The rational utilization and sustainable development of energy are the hotspots of current research. This paper briefly introduces the current control method of the parallel loop of the inverter power supply. Then, three difficulties in the parallel operation of the inverter power supply are summed up, namely, the asynchronous voltage frequency and voltage phase of inverter power supply, the inconsistent amplitude of output voltage, and the influence of the difference of harmonic components in voltage. Besides, the present work discusses the current sharing control scheme of a traditional parallel system and proposes three current sharing control methods. The optimization methods of the main circuit topology, droop parallel control, and dynamic adjustment of the unit inverter are designed based on the above analysis. Finally, simulation experiments are designed to verify its performance. The experimental results show that the control strategy proposed here has significantly improved the system's dynamic performance and steady-state index. The simulation model of the parallel wireless inverter system established here provides an experimental platform for future system theory research. There is still power coupling and unequal active power sharing due to inconsistent line impedance and mismatched inverter capacity in a low-voltage microgrid. Introducing the virtual impedance can realize the decoupling control of the power in the system; however, the increase of the equivalent output impedance of the system may reduce the system voltage. The improved droop control strategy proposed here can offset

the equivalent output impedance of the parallel inverter system by designing the value of virtual complex impedance to realize the purely resistive system impedance and the decoupling control of active power and reactive power.

Due to the limitation of the research capacity and research funds, the inverter design based on multiobjective decision-making reported here is not ideal. Moreover, in the open-circuit parallel system under droop control, the voltage and frequency change with the load, which affects the power supply quality. Dynamic compensation can eliminate some effects, but the effect cannot adapt to all practical applications. Follow-up research will improve these two points to enhance the value and reliability of the present work.

## Data Availability

The labeled dataset used to support the findings of this study are available from the corresponding author upon request.

## Conflicts of Interest

The author declares no competing interests.

## Acknowledgments

This research was supported by the project of Science and Technology Research Program of Chongqing Municipal Education Commission of China (Grant No. KJQN201901607), Chongqing Big Data Engineering Laboratory for Children, Chongqing Electronics Engineering Technology Research Center for Interactive Learning, Chongqing University Innovation Research Group, Chongqing Key Discipline of Electronic Information, Chongqing Natural Science Foundation Project (CSTC2021-msxm1993), and the Science and Technology Research Program of Chongqing Municipal Education Commission (Grant No. KJZD-M201801601).

## References

[1] P. Herasymenko, "Mathematical analysis of dual-frequency load current of two-inverter power supply for induction heating systems," *Przegląd Elektrotechniczny*, vol. 1, no. 3, pp. 71–76, 2021.

[2] D. Dietz, "Stochastic propagation delay through a CMOS inverter as a consequence of stochastic power supply voltage—part II: modeling examples," *IEEE Transactions on Electromagnetic Compatibility*, vol. 61, no. 1, pp. 233–241, 2019.

[3] J. K. Sahani, A. Singh, and A. Agarwal, "A wide frequency range low jitter integer PLL with switch and inverter based CP in 0.18 $\mu$m CMOS technology," *Journal of Circuits, Systems, and Computers*, vol. 29, no. 9, pp. 167–170, 2020.

[4] S. Xu, B. Yang, and D. Li, "Analysis on the applicability of phase selection components of inverter power supply transmission line," *E3S Web of Conferences*, vol. 204, no. 13, 2020.

[5] V. B. Ivanov, "Modeling of three-phase inverter power supply system in Simulink," *IOP Conference Series Materials Science and Engineering*, vol. 1032, no. 1, article 012054, 2021.

[6] N. A. Windarko, A. Puryanto, R. P. Eviningsih, M. Z. Efendi, E. Prasetyono, and B. Sumantri, "Prototipe power supply gate driver untuk multilevel inverter dengan menggunakan flyback converter multi output," *Techné: Jurnal Ilmiah Elektroteknika*, vol. 19, no. 1, pp. 33–42, 2020.

[7] C. Liu, S. H. Chang, Y. J. Chen et al., "A power supply consists of the DC-DC boost converter and a full-bridge inverter circuits for a PZT liquid pump," *International Journal of Information and Electronics Engineering*, vol. 9, no. 1, pp. 19–22, 2019.

[8] G. Zhang, Z. Tian, P. Tricoli, S. Hillmansen, Y. Wang, and Z. Liu, "Inverter operating characteristics optimization for DC traction power supply systems," *IEEE Transactions on Vehicular Technology*, vol. 68, no. 4, pp. 3400–3410, 2019.

[9] M. A. Hannan, Z. A. Ghani, M. M. Hoque, and M. S. Hossain Lipu, "A fuzzy-rule-based PV inverter controller to enhance the quality of solar power supply: experimental test and validation," *Electronics*, vol. 8, no. 11, 2019.

[10] H. F. Baghtash, "Bias-stabilized inverter-amplifier: an inspiring solution for low-voltage and low-power applications," *Analog Integrated Circuits and Signal Processing*, vol. 105, no. 3, pp. 1–6, 2020.

[11] S. Kundu, S. Banerjee, and S. Bhowmick, "Improved SHM-PAM-based five-level CHB inverter to fulfil NRS 048-2:2003 grid code and to apply as shunt active power filter with tuned proportional-resonant controller for improving power quality," *IET Power Electronics*, vol. 13, no. 11, pp. 2350–2360, 2020.

[12] S. Somkun, "Unbalanced synchronous reference frame control of singe-phase stand-alone inverter," *International Journal of Electrical Power & Energy Systems*, vol. 107, pp. 332–343, 2019.

[13] L. Lin, G. Qian, H. Jian, and M. Hao, "An enhanced power sharing strategy for islanded microgrids using adaptive virtual impedances," in *IECON 2015-41st Annual Conference of the IEEE Industrial Electronics Society*, Yokohama, Japan, 2016.

[14] Z. Peng, J. Wang, D. Bi et al., "Droop control strategy incorporating coupling compensation and virtual impedance formicrogrid application," *IEEE Transactions on Energy Conversion*, vol. 34, no. 1, pp. 277–291, 2019.

[15] Z. Chen, X. J. Pei, M. Yang, and L. Peng, "An adaptive virtual resistor (AVR) control strategy for low-voltage parallel inverters," *IEEETransactions on Power Electronics*, vol. 34, no. 1, pp. 863–876, 2019.

[16] J. Y. Zhang, J. Shu, J. Ning, L. Huang, and H. Wang, "Enhanced proportional power sharing strategy based on adaptive virtual impedance in low-voltage networked microgrid," *IET Generation Transmission & Distribution*, vol. 12, no. 11, pp. 2566–2576, 2018.

[17] Y. M. Geng, M. Y. Hou, and G. F. Zhu, "Resistive droop control strategy of active power distribution for microgrid based on virtual impedance," *Electric Power Automation Equipment*, vol. 40, no. 10, pp. 132–138, 2020.

[18] T. Liu, B. G. Guan, and Y. F. Liang, "Ring current suppression strategy between island microgrid parallel inverters based on virtual impedance," *Intelligent Computer and Application*, vol. 10, no. 1, pp. 160–164, 2020.

[19] G. Gao, J. Zeng, J. Han, and X. Lei, "Design of backstepping controller for T-type network inverter," *IOP Conference Series Earth and Environmental Science*, vol. 467, no. 1, article 012030, 2020.

[20] W. Lai, W. Chen, J. Li, X. Zhang, Z. Lin, and H. Li, "Nonlinear adaptive control of PV inverter for maximum solar energy harvesting using democratic joint," *IOP Conference Series: Earth and Environmental Science*, vol. 467, no. 1, article 012068, 2020.

[21] G. Feng, P. Wang, H. X. Liang, K. Yu, and X. Zeng, "Arc suppression method for distribution network with new energy based on active inverter split-phase injection," *IOP Conference Series Earth and Environmental Science*, vol. 495, no. 1, article 012025, 2020.

[22] D. Ma, K. Cheng, R. Wang, S. Lin, and X. Xie, "The decoupled active/reactive power predictive control of quasi-Z-source inverter for distributed generations," *International Journal of Control, Automation and Systems*, vol. 19, no. 2, pp. 810–822, 2021.

[23] D. Ghaderi, S. Padmanaban, P. K. Maroti, B. Papari, and J. B. Holm-Nielsen, "Design and implementation of an improved sinusoidal controller for a two-phase enhanced impedance source boost inverter," *Computers & Electrical Engineering*, vol. 83, no. 2020, article 106575, 2020.

[24] Q. Chen, J. Pan, S. Liu, G. Chen, and J. Xiong, "New type single-supply four-switch five-level inverter with frequency multiplication capability," *IEEE Access*, vol. 8, pp. 203347–203357, 2020.

[25] F. Gonzalez-Hernando, J. San-Sebastian, A. Garcia-Bediaga, M. Arias, F. Iannuzzo, and F. Blaabjerg, "Wear-out condition monitoring of IGBT and mosfet power modules in inverter operation," *IEEE Transactions on Industry Applications*, vol. 55, no. 6, pp. 6184–6192, 2019.

[26] J. Rąbkowski, H. Skoneczny, R. Kopacz, P. Trochimiuk, and G. Wrona, "A simple method to validate power loss in medium voltage SiC MOSFETs and Schottky diodes operating in a three-phase inverter," *Energies*, vol. 13, no. 18, 2020.

[27] M. G. Varzaneh, A. Rajaei, A. Jolfaei, and M. R. Khosravi, "A high step-up dual-source three phase inverter topology with decoupled and reliable control algorithm," *IEEE Transactions on Industry Applications*, vol. 56, no. 4, pp. 4501–4509, 2020.

[28] P. Mishra, A. K. Pradhan, and P. Bajpai, "Voltage control of PV inverter connected to unbalanced distribution system," *IET Renewable Power Generation*, vol. 13, no. 9, pp. 1587–1594, 2019.

[29] Y. Li, Y. Wei, Q. Wang, Y. Huang, and J. Cheng, "Design method of high efficiency class-E inverter applied to magnetic coupled resonant wireless power transmission system," *Diangong Jishu Xuebao/Transactions of China Electrotechnical Society*, vol. 34, no. 2, pp. 219–225, 2019.

[30] S. K. Kim, "Performance-recovery proportional-type output-voltage tracking algorithm of three-phase inverter for uninterruptible power supply applications," *IET Circuits, Devices & Systems*, vol. 13, no. 2, pp. 185–192, 2019.

[31] T. Roy, N. Aarzoo, P. K. Sadhu, and A. Dasgupta, "A novel three-phase multilevel inverter structure using switched capacitor basic unit for renewable energy conversion systems," *International Journal of Power Electronics*, vol. 10, no. 1/2, pp. 133–154, 2019.

[32] D. T. Nugroho and T. Noguchi, "A different voltage-source power inverter with carrier based SPWM for open-end connection loads," *Energies*, vol. 12, no. 17, 2019.

[33] D. Çelik, M. E. Meral, and M. Inci, "Virtual Park-based control strategy for grid-connected inverter interfaced renewable energy sources," *IET Renewable Power Generation*, vol. 13, no. 15, pp. 2840–2852, 2019.

[34] J. Choi, A. Khalsa, D. A. Klapp, S. Baktiono, and M. S. Illindala, "Survivability of prime-mover powered inverter-based distributed energy resources during microgrid islanding," *IEEE Transactions on Industry Applications*, vol. 55, no. 2, pp. 1214–1224, 2019.

[35] M. Parvez, M. F. M. Elias, N. A. Rahim, F. Blaabjerg, D. Abbott, and S. F. Al-Sarawi, "Comparative study of discrete PI and PR controls for single-phase UPS inverter," *IEEE Access*, vol. 8, pp. 45584–45595, 2020.

[36] A. Ali, M. A. Sayed, and T. Takeshita, "Isolated single-phase single-stage DC-AC cascaded transformer-based multilevel inverter for stand-alone and grid-tied applications," *International Journal of Electrical Power & Energy Systems*, vol. 125, 2021.